Published in final edited form as:
Science. 2013 April 12; 340(6129): 202–207. doi:10.1126/science.1235208.

Blockade of Chronic Type I Interferon Signaling to Control Persistent LCMV Infection

Elizabeth B. Wilson[1], **Douglas H. Yamada**[1], **Heidi Elsaesser**[1], **Jonathan Herskovitz**[1], **Jane Deng**[2], **Genhong Cheng**[1], **Bruce J. Aronow**[3], **Christopher L. Karp**[4,*], and **David G. Brooks**[1,†]

[1]Department of Microbiology, Immunology and Molecular Genetics and the UCLA AIDS Institute, David Geffen School of Medicine, University of California, Los Angeles (UCLA), Los Angeles, CA 90095, USA

[2]Division of Pulmonary and Critical Care Medicine, David Geffen School of Medicine, UCLA, Los Angeles, CA 90095, USA

[3]Division of Biomedical Informatics and Division of Developmental Biology, Cincinnati Children's Hospital Research Foundation and the University of Cincinnati College of Medicine, Cincinnati, OH 45267, USA

[4]Division of Molecular Immunology, Cincinnati Children's Hospital Research Foundation and the University of Cincinnati College of Medicine, Cincinnati, OH 45267, USA

Abstract

Type I interferons (IFN-I) are critical for antiviral immunity; however, chronic IFN-I signaling is associated with hyperimmune activation and disease progression in persistent infections. We demonstrated in mice that blockade of IFN-I signaling diminished chronic immune activation and immune suppression, restored lymphoid tissue architecture, and increased immune parameters associated with control of virus replication, ultimately facilitating clearance of the persistent infection. The accelerated control of persistent infection induced by blocking IFN-I signaling required CD4 T cells and was associated with enhanced IFN-γ production. Thus, we demonstrated that interfering with chronic IFN-I signaling during persistent infection redirects the immune environment to enable control of infection.

Despite initially robust antiviral immune activity, some viruses, including HIVand hepatitis C virus (HCV) in humans and lymphocytic choriomeningitis virus (LCMV) in mice, outpace the immune response and establish persistent infections (1, 2). Besides virus-mediated evasion tactics, the host initiates an immunosuppressive program that actively suppresses antiviral T cell responses and facilitates persistent infection (3–8). The expression of suppressive factors is tightly linked to viral burden (3, 4, 8), suggesting the presence of an immunologic sensory system that continually measures the magnitude and duration of viral replication and then dynamically modulates the balance between antiviral immunity and immune exhaustion.

In order to identify the mechanisms orchestrating the immunosuppressive program during virus infection, we performed RNA microarray–based splenic network analysis. We compared mice infected with one of two LCMV strains: the Armstrong (Arm) strain, which induces a robust T cell response that resolves infection within 8 to 10 days, or the clone 13

†Corresponding author. dbrooks@microbio.ucla.edu.
*Present address: The Bill and Melinda Gates Foundation, Seattle, WA 98109, USA.

Supplementary Materials www.sciencemag.org/cgi/content/full/340/6129/202/DC1

(Cl13) strain, which generates a persistent infection because of the sustained expression of an immunosuppressive program, including production of inter-leukin (IL)-10 and expression of the inhibitory molecule PD-L1 (programmed cell death 1 ligand 1) (4, 5, 9–13). PD-L1 and IL-10 are similarly expressed at the onset of both acute and persistent infection; however, expression of these molecules wanes with resolution of acute infection, whereas they are maintained or elevated in persistent infection (3, 4, 8). Similarly, antigen-presenting cell (APC) populations expressing multiple suppressive factors with the ability to inhibit Tcell responses are present early in acute infection but are elevated in the context of persistent infection (8). We focused our microarray analysis to identify factors exhibiting a similar kinetic that might be used to sense virus replication dynamics and control immunosuppressive programs. Tissue-wide cytokine expression patterns were similar in acute and persistent infections (fig. S1A). However, analogous to virus clearance kinetics, type I inter-feron (IFN-I) receptor (IFNR)–stimulated genes, signal transducer and activator of transcription (STAT) genes, and IFN-I regulatory factors were initially similarly expressed in LCMV-Arm and LCMV-Cl13 infections but then rapidly dissipated as acute LCMV-Arm infection resolved, whereas they remained elevated in LCMV-Cl13 infection (Fig. 1A and table S1). In total spleen, the expression of IFN-α and IFN-β was not elevated above uninfected mice (fig. S1B); however, at day 9 postinfection IFN-α and IFN-β transcripts were still present in dendritic cells (DCs) from LCMV-Cl13–infected mice (Fig. 1B). Analysis of IL-10–green fluorescent protein (GFP) (Vert-X) reporter mice (8, 14) revealed that *OAS* and *Mx1* (genes directly stimulated by IFNR signaling) expression levels were specifically enriched in the immunoregulatory APCs that co-express the highest levels of PD-L1 and IL-10 and can suppress antiviral T cell responses (8) (Fig. 1C), suggesting a link between prolonged IFN-I signaling and immunosuppression. Expression of *IRF3*, a gene involved in the IFN-I response but whose expression is not directly regulated by IFNR signaling (15), was not differentially increased in immunoregulatory APCs (Fig. 1C).

We next determined the impact of IFN-I signaling on the immunosuppressive program in vivo. Although levels of virus replication usually correlate with expression of suppressive factors (1), *Ifnar1*$^{-/-}$ mice exhibited decreased expression of PD-L1 and IL-10 compared with wild-type mice at day 9 after LCMV-Cl13 infection (Fig. 2A and fig. S2A) despite elevated levels of viral replication and viral antigen (fig. S2, A and B). Furthermore, treatment of splenocytes with IFNβ stimulated increased PD-L1 and IL-10 expression (fig. S2C). Taken together, these data suggest that IFN-I signaling drives the immunosuppressive program in vivo. *Ifnar1*$^{-/-}$mice failed to clear LCMV-Arm by day 9 after infection (fig. S2D), consistent with the antiviral and immune stimulatory effect of IFN-I during viral infection (16).

To resolve the role of IFN-I in induction of the immunosuppressive program separate from potential abnormalities of life-long genetic deficiency in *Ifnar1*$^{-/-}$ mice (17), we treated wild-type mice with an IFNR1-blocking antibody beginning 1 day before LCMV-Cl13 infection. IFNR1 blockade diminished *Mx1*, *OAS*, and *IRF7* expression in multiple tissues and cell types (fig. S3A), indicating the ability to inhibit IFN-I signaling in vivo. Analogous to persistently infected *Ifnar1*$^{-/-}$ mice, IFNR1 antibody blockade led to decreased PD-L1 and IL-10 expression and elevated virus titers compared with isotype antibody–treated LCMV-Cl13–infected mice on day 9 after infection (Fig. 2B). IL-10 levels rebounded when IFNR1 blocking antibody treatment was withdrawn (day 15; Fig. 2B), indicating sensitive surveillance and rapid modulation of the immunosuppressive state through IFN-I signaling. Heightened IFN-I signaling can inhibit inflammasome activity in some situations (18). However, despite higher levels of virus replication and LCMV antigen in splenic APCs from persistently infected mice treated with IFNR1 blocking antibody (Fig. 2B and fig. S2B), reduced amounts of IL-1, IL-18, and inflammasome activation were observed (fig. S3B), indicating that blockade of IFN-I signaling decreases chronic inflammation during persistent

infection. The reduced levels of inhibitory factors and chronic activation after IFNR1 blockade were not indicative of global down-regulation of pro-inflammatory cytokines, and in fact expression of IFN-γ, a factor critical for control and therapeutic resolution of persistent LCMV infection (16, 19, 20), was elevated after IFNR1 blockade (fig. S3B). Thus, IFNR blockade during persistent infection diminishes immunosuppressive signals and chronic inflammation during persistent infection.

IFNR1 antibody blockade before infection also decreased the level of IL-10– and PD-L1–expressing immunoregulatory DCs (Fig. 2C), leading to an enhanced ratio of stimulatory to immunoregulatory DCs. Moreover, IFNR1 antibody blockade prevented the splenic disorganization associated with impaired immune cell interactions and the inability to control persistent infection (21–23) (Fig. 2D and fig. S3C). Thus, immune cells are likely better positioned to interact with one another, and, because of the decrease in immunoregulatory DC frequency, those interactions are more likely to be stimulatory.

We next determined how blockade of IFN-I signaling before infection contributed to control of persistent infection. Although virus titers were initially increased in mice treated with IFNR1 blocking antibody, by 30 days postinfection viremia was reduced compared with isotype treatment, and many of the mice had already controlled infection (Fig. 3A). Furthermore, virus titers were decreased in multiple compartments, including the kidney (a life-long reservoir of LCMV-Cl13) (Fig. 3B). Mirroring findings in *Ifnar1*$^{-/-}$ mice (16), IFNR1 blockade in wild-type mice led to persistent infection with LCMV-Arm (fig. S2D), demonstrating the antiviral activity of IFN-I and its requirement to control acute viral infection.

We next sought to understand the immune mechanisms through which IFNR1 blockade enables control of persistent viral infection. IFNR1 blockade before infection induced a numerical increase in many immune subsets 9 days after infection including the total number of functional virus-specific CD4 Tcells (Fig. 3C and fig. S4A). However, despite an overall increase in B cells and CD4 T cells, LCMV-specific antibody titers were not elevated in IFNR1 blocking antibody–treated mice at day 9 or 30 after infection (fig. S4B). Unlike virus-specific CD4 T cells, virus-specific CD8 T cell numbers and cytokine production were similar or slightly reduced when IFN-I signaling was blocked (Fig. 3C and fig. S4C). On the basis of the increase in natural killer (NK) cells, virus-specific CD4 T cells, and systemic IFN-γ levels (Fig. 3C and figs. S3B and S4A), we sought to examine the role of each of these factors in accelerating virus clearance after IFNR1 blockade. CD4 depletion before infection abrogated the accelerated virus control engendered by IFNR1 blockade, whereas NK cell depletion did not affect IFNR1 blockade–mediated clearance (Fig. 3D). To assess the role of increased IFN-γ in IFNR1 blockade–induced virus clearance, we treated mice with IFNR1 blocking antibody with or without IFN-γ blocking antibodies at the time of LCMV-Cl13 infection. The accelerated clearance of persistent infection after IFNR1 blockade was abrogated in mice cotreated with IFN-γ blocking antibody (anti–IFN-γ) (Fig. 3E). Although occurring later than in IFN-γ knockout mice (24), mice treated with anti–IFN-γ alone died ~35 days after infection, whereas mice receiving IFNR1 blocking antibody plus anti–IFN-γ survived and cleared infection similar to untreated mice. Together, these results indicate that IFNR1 antibody stimulates accelerated clearance of persistent virus infection through CD4 T cell and IFN-γ–dependent mechanisms.

We next determined whether therapeutic blockade of IFN-I signaling affected an established LCMV-Cl13 infection. Blockade of IFNR1 beginning 25 days after infection accelerated control of persistent infection in multiple compartments compared with isotype treatment (Fig. 4, A and B). The enhanced control of infection occurred despite the initial increase in

virus titers immediately after IFNR1 blocking antibody therapy (Fig. 4A). Blockade of IFNR1 beginning 25 days after infection reduced the IFN-I gene expression signature and decreased IL-10 and PD-L1 levels (Fig. 4, C and D), demonstrating that IFN-I continues to be a key component of an immunologic surveillance system and stimulator of the immunosuppressive program throughout persistent infection. Thus, therapeutically ablating chronic IFN-I immune activation in vivo enhances control of persistent LCMV infection.

Our results demonstrate that chronic IFN-I signaling during persistent infection drives the immunosuppressive program and that interfering with IFN-I signaling restores multiple parameters of productive immunity, allowing for viral clearance. IFN-I treatment in combination with the antiviral drug ribavirin is often effective at eradicating HCV infection. However, some patients fail to have a sustained virologic response. A characteristic of patients that fail IFN-I/ribavirin therapy is a heightened IFN-I signature before treatment that fails to substantially increase with therapy (25, 26). Thus, the initially high IFN-I signature may lead to enhanced immune dysfunction, and consequently adding more IFN-I is ineffective. These results highlight the duality of IFN-I during viral infection: Acute IFN-I signals possess antiviral and immune stimulatory potential required for clearance of infection, but when virus cannot be controlled, acutely sustained IFN-I signaling induces immunosuppression that facilitates persistent virus infection. Considering that HIV and HCV infections are also associated with immune activation driven by chronic IFN-I signaling (23, 27–29), a similar blockade of IFN-I may improve control of these infections. In total, our data support IFN-I as a central rheostat and regulator of the immunosuppressive program and the possibility that it may be feasible to redirect entire immunologic programs by modulating activity of a single pathway: IFN-I.

Supplementary Material

Refer to Web version on PubMed Central for supplementary material.

Acknowledgments

We thank S. Bensinger for insightful discussion and critical review of the manuscript, all the members of the Brooks laboratory for discussions and technical assistance, and the UCLA Translational Pathology Core Facility for expert histological tissue processing and analysis. The data presented in the manuscript are tabulated in the main paper and in the supplementary materials. D.G.B. and E.B.W. are named inventors on a provisional patent assigned to The Regents of the University of California relating in part to methods of treating chronic viral infections by administering agents that inhibit IFN. The microarray data set from this study is available at www.ncbi.nlm.nih.gov/geo/(accession no. GSE44322). Our work was supported by the NIH (grants AI085043 and AI082975 to D.G.B., AI060567 to E.B.W., and HL108949 to J.D.), an Institutional Clinical and Translational Science Award (NIH/NCATS 8UL1TR000077-04 to B.J.A.), and the UCLA Center for AIDS Research (P30 AI028697).

References and Notes

1. Wilson EB, Brooks DG. Immunol. Res. 2010; 48:3. [PubMed: 20725865]
2. Li Q, et al. Science. 2009; 323:1726. [PubMed: 19325114]
3. Barber DL, et al. Nature. 2006; 439:682. [PubMed: 16382236]
4. Brooks DG, et al. Nat. Med. 2006; 12:1301. [PubMed: 17041596]
5. Ejrnaes M, et al. J. Exp. Med. 2006; 203:2461. [PubMed: 17030951]
6. Day CL, et al. Nature. 2006; 443:350. [PubMed: 16921384]
7. Brockman MA, et al. Blood. 2009; 114:346. [PubMed: 19365081]
8. Wilson EB, et al. Cell Host Microbe. 2012; 11:481. [PubMed: 22607801]
9. Clerici M, et al. J. Clin. Invest. 1994; 93:768. [PubMed: 8113410]
10. Landay AL, et al. J. Infect. Dis. 1996; 173:1085. [PubMed: 8627058]

11. Rigopoulou EI, Abbott WG, Haigh P, Naoumov NV. Clin. Immunol. 2005; 117:57. [PubMed: 16006191]
12. Brockman MA, et al. Blood. 2009; 114:346. [PubMed: 19365081]
13. Flynn JK, et al. ATAHC Study Group. J. Viral Hepat. 2011; 18:549. [PubMed: 20626625]
14. Madan R, et al. J. Immunol. 2009; 183:2312. [PubMed: 19620304]
15. Au WC, Moore PA, Lowther W, Juang YT, Pitha PM. Proc. Natl. Acad. Sci. U.S.A. 1995; 92:11657. [PubMed: 8524823]
16. Müller U, et al. Science. 1994; 264:1918. [PubMed: 8009221]
17. Gough DJ, Messina NL, Clarke CJ, Johnstone RW, Levy DE. Immunity. 2012; 36:166. [PubMed: 22365663]
18. Guarda G, et al. Immunity. 2011; 34:213. [PubMed: 21349431]
19. Tishon A, Lewicki H, Rall G, Von Herrath M, Oldstone MB. Virology. 1995; 212:244. [PubMed: 7676639]
20. Von Herrath MG, Coon B, Oldstone MB. Virology. 1997; 229:349. [PubMed: 9126248]
21. Tishon A, Borrow P, Evans C, Oldstone MB. Virology. 1993; 195:397. [PubMed: 8393233]
22. Müller S, et al. J. Virol. 2002; 76:2375. [PubMed: 11836415]
23. Moir S, Chun TW, Fauci AS. Annu. Rev. Pathol. 2011; 6:223. [PubMed: 21034222]
24. Ou R, Zhou S, Huang L, Moskophidis D. J. Virol. 2001; 75:8407. [PubMed: 11507186]
25. Chen L, et al. Gastroenterology. 2005; 128:1437. [PubMed: 15887125]
26. Sarasin-Filipowicz M, et al. Proc. Natl. Acad. Sci. U.S.A. 2008; 105:7034. [PubMed: 18467494]
27. Bosinger SE, et al. J. Clin. Invest. 2009; 119:3556. [PubMed: 19959874]
28. Jacquelin B, et al. J. Clin. Invest. 2009; 119:3544. [PubMed: 19959873]
29. Bolen CR, et al. J. Interferon Cytokine Res. 2013; 33:15. [PubMed: 23067362]

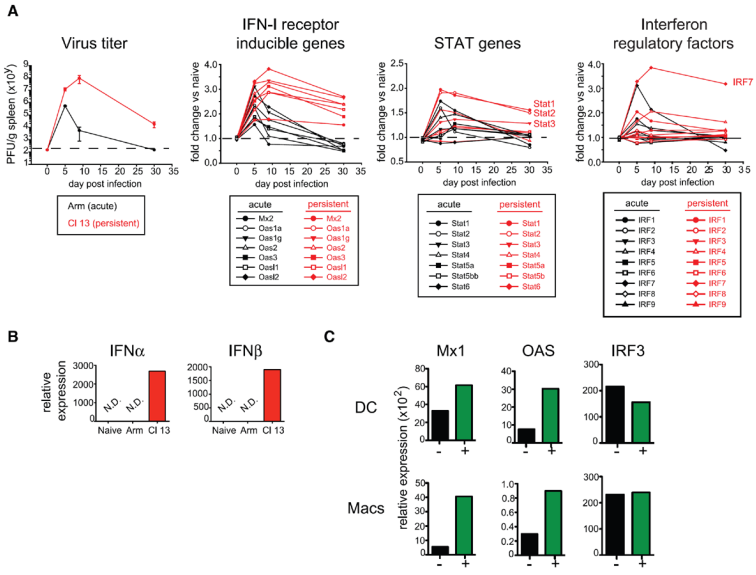

Fig. 1. Prolonged IFN-I signaling during persistent infection

(**A**) Splenic virus titers ± SD after acute LCMV-Arm (black) and persistent LCMV-Cl13 (red) infection (left). Gene expression kinetics by microarray analysis of the indicated IFNR-inducible, STAT, and IFN-I regulatory factors (IRFs) in whole spleen tissue after LCMV-Arm (black) or LCMV-Cl13 (red) relative to naïve (uninfected) mice. Each value indicates the average of three to four mice per group per time point. Values are shown without error bars for clarity, and the *P* values for each gene are indicated in table S1. PFU, plaque-forming units. (**B**) *IFN*α (left) and *IFN*β (right) mRNA expression relative to a control gene, *HPRT*, in splenic DCs from naïve or LCMV-Arm– or LCMV-Cl13–infected mice (day 9). N.D. indicates that *IFN*α or *IFN*β transcripts were not detected after 40 cycles of amplification. *HPRT* mRNA expression was measurable in all samples. (**C**) *Mx1, OAS*, and *IRF3* mRNA expression relative to *HPRT* in the indicated IL-10+ (GFP+, green) or IL-10− (GFP−, black) splenic DCs (top) or macrophages (bottom) 9 days after LCMV-Cl13 infection of Vert-X IL-10 reporter mice. For (B) and (C), each group is a pool of cells from six to eight mice and is representative of two independent experiments.

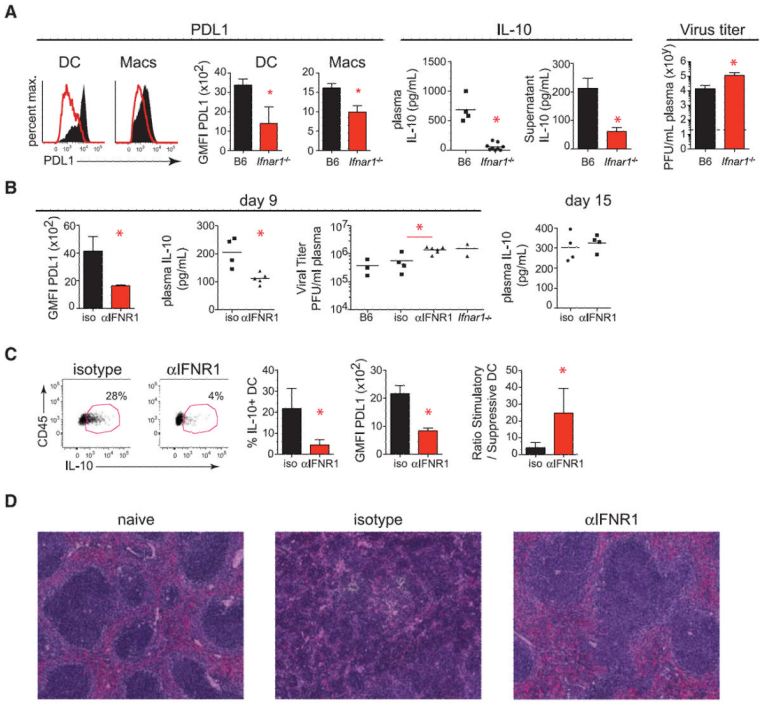

Fig. 2. The immunosuppressive program during persistent infection is dependent on IFN-I signaling

(**A**) Representative histograms and summarized quantification of geometric mean fluorescence intensity (GMFI) show PD-L1 on splenic DCs and macrophages 9 days after LCMV-Cl13 infection in wild-type (WT, black) and *Ifnar1*$^{-/-}$ (red) mice. Scatter plots show plasma IL-10 levels on day 9 after LCMV-Cl13 infection. Bar graphs measure IL-10 production by cultured splenocytes (in the absence of exogenous stimulation) isolated 9 days after LCMV-Cl13 infection from WT or *Ifnar1*$^{-/-}$ mice. Plasma viral titers in WT or *Ifnar1*$^{-/-}$ mice on day 9 after LCMV-Cl13 infection are shown to the far right. Dashed lines indicate the level of detection of the plaque assay (200 PFU). (B to D) WT mice were treated with isotype or IFNR1 blocking antibody beginning 1 day before LCMV-Cl13 infection. (**B**) Graphs indicate GMFI of PD-L1 on splenic CD45+ cells (left), plasma levels of IL-10 (middle), and plasma viral titers (right) of untreated mice (B6), isotype-treated mice, IFNR1 blocking antibody (αIFNR1)–treated mice, and untreated *Ifnar1*$^{-/-}$ mice. Plasma IL-10 levels on day 15 after LCMV-Cl13 infection are shown on the far right. (**C**) Flow cytometry plots of IL-10 reporter expression (GFP) in splenic DCs from Vert-X mice treated with isotype or IFNR1 blocking antibody. Bar graphs show the frequency of IL-10 expression and the GMFI of PD-L1 expression by splenic DCs. The ratio of IL-10–nonproducing to IL-10–producing DCs is shown on the far right. (**D**) Hematoxylin and eosin staining of spleens from naïve mice (left) or on day 9 after LCMV-Cl13 infection of mice treated with isotype (middle) or IFNR1 blocking antibody (right). Symbols represent individual mice with bars indicating the mean of the group. In bar graphs, the data represent the average ± SD of three to six mice per group. All data are representative of two or more independent experiments. **P* < 0.05.

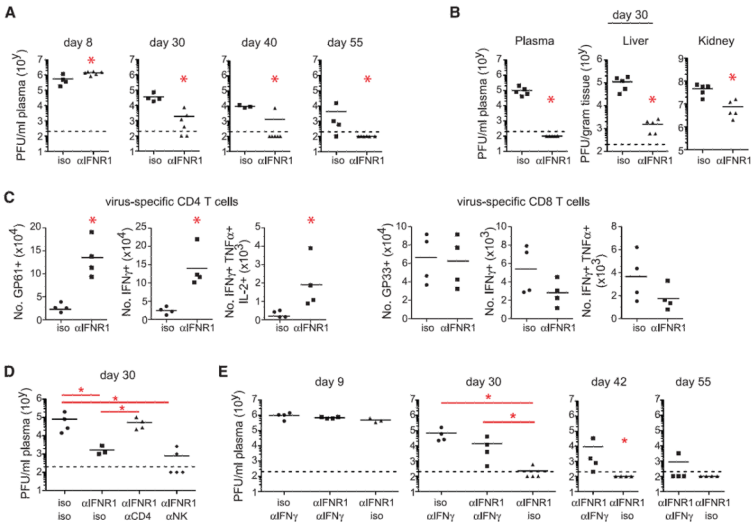

Fig. 3. IFNR1 blockade enhances control of persistent infection

WT mice were treated with isotype or IFNR1 blocking antibody beginning 1 day before LCMV-Cl13 infection. (**A**) Plasma virus titers at the indicated time points after infection. (**B**) Viral titers in plasma, liver, and kidney 30 days after infection. (**C**) Graphs indicate total numbers of IFN-γ–expressing and of multicytokine-producing (polyfunctional) LCMV-$GP_{61–80}$–specific CD4 T cells and LCMV-$GP_{33–41}$–specific CD8 T cells. (**D**) Plasma viral titers at day 30 after LCMV-Cl13 infection in mice that were either undepleted of cells and treated with isotype (iso/iso) or IFNR1 (αIFNR1/iso) blocking antibody or depleted of CD4 T cells (αCD4) or NK cells (αNK) before infection and IFNR1 blocking antibody treatment. (**E**) Plasma virus titers at the indicated time point after LCMV-Cl13 infection in mice that were either treated with isotype or IFNR1 blocking antibody with or without anti–IFN-γ (αIFN-γ). *x* axis labels indicate (top) IFNRI or isotype and (bottom) cell or IFN-γ depleting antibody treatments. Each symbol in the scatter plots represents an individual mouse with bars indicating the mean of the group. Dashed lines indicate the level of detection of the plaque assay (200 PFU). Data are representative of two or more independent experiments. $*P < 0.05$.

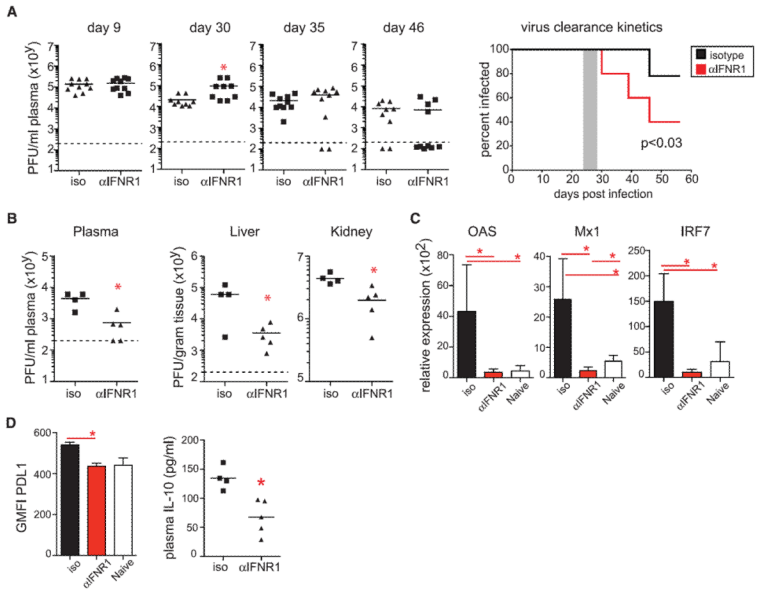

Fig. 4. Therapeutic IFNR1 antibody blockade dampens the immunosuppressive program and facilitates clearance of persistent infection

WT mice were treated with isotype or IFNR1 blocking antibody beginning on day 25 after LCMV-Cl13 infection. (**A**) Plasma viral titers at the indicated time points. The percent of mice at each time point exhibiting detectible virus titers is summarized in the kinetic graph to the right, with the shaded area representing the time of treatment. The data are combined from two experiments. (**B**) Viral titers in the plasma, liver, and kidney at day 46 after LCMV-Cl13 infection. (**C**) *OAS, Mx1*, and *IRF7* mRNA expression relative to *HPRT* in splenocytes from naïve mice (white) or on day 30 after LCMV-Cl13 infection in mice treated with isotype (black) or IFNR1 (red) blocking antibody. (**D**) Graphs indicate GMFI of PD-L1 on splenic dendritic cells (left) and plasma IL-10 levels (right) on day 30 after LCMV-Cl13 infection in mice treated with isotype or IFNR1 blocking antibody. Each symbol in the scatter plot represents an individual mouse, and bar graphs indicate the average value ± SD. All data are representative of two to five independent experiments. **P* < 0.05.